國立臺灣科技大學

TAIWAN TECH

National Taiwan University
of Science and Technology

BME Graduate Program and Research Overview

Chairman：Ching-Wei, WANG
Graduate Institute of Biomedical Engineering
College of Applied Sciences
2024/10/24



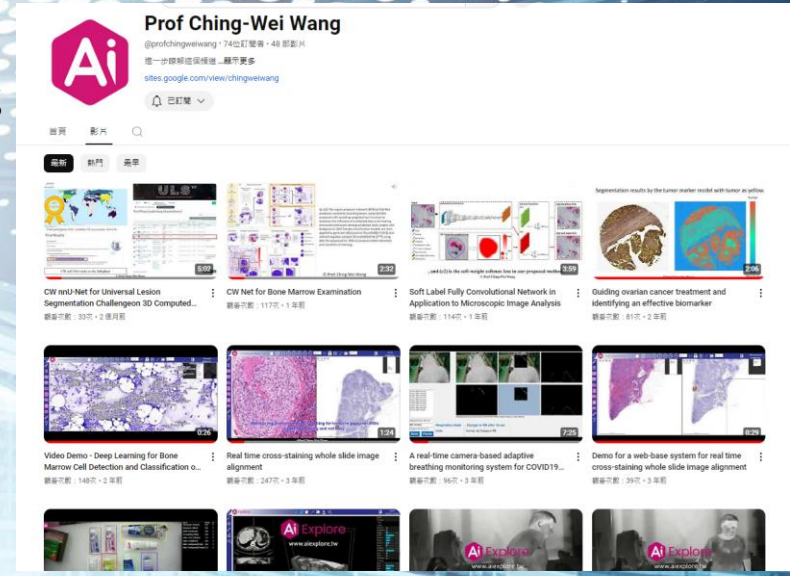
CHAIRMAN OF GRADUATE INSTITUTE OF BIOMEDICAL ENGINEERING



Research Interests：

· Deep Learning and Machine Learning
· Terapixel AI Cloud System / Big Data Analysis
· Pathology AI and Cytology AI
· Medical Image Analysis
· Computer Vision and Image Processing

World's Top 2% Scientists



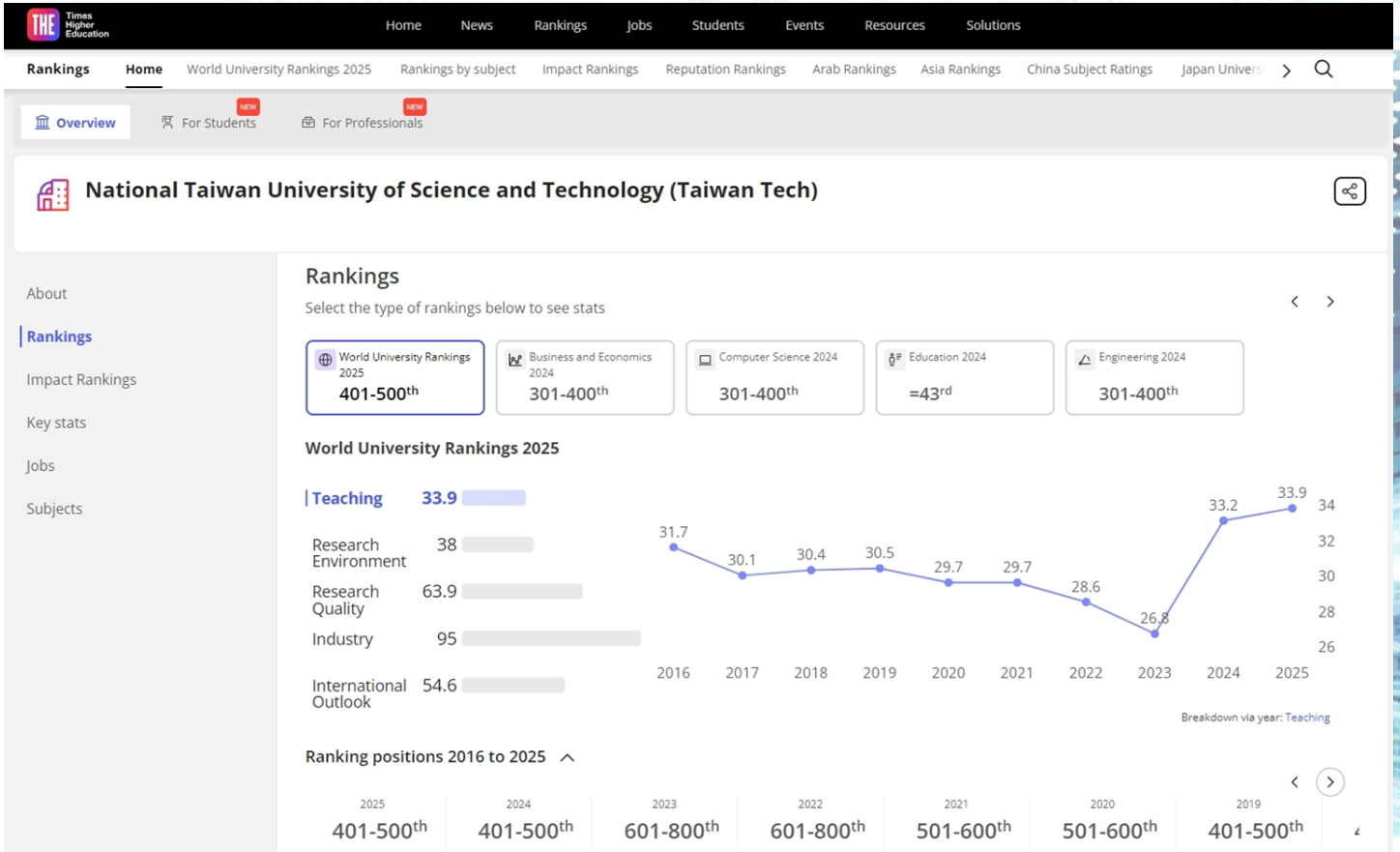
Prof. Dr. Ching-Wei Wang (cweiwang@mail.ntust.edu.tw)
Publication (Google Scholar, ORCID, Scopus))
YouTube GitHub AI Projects
Director, Graduate Institute of Biomedical Engineering
National Taiwan University of Science and Technology
https://sites.google.com/view/chingweiwang

Education：

· PhD in Computer Science, University of Lincoln, Lincoln, UK, 2005/12/1-2009/3/30
· MSc with Distinction, IT(System and Software), University of Glasgow, Glasgow, UK, 2002/9/1-2003/9/1

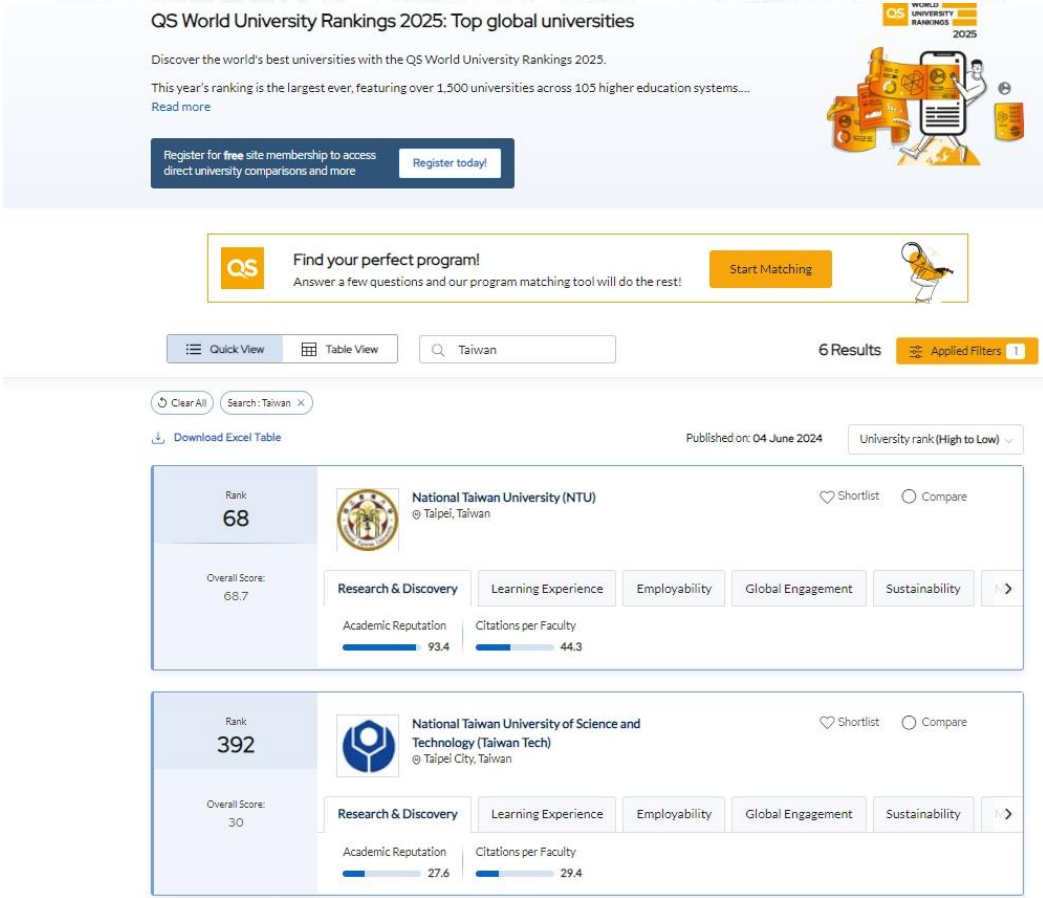
TAIWAN TECH
NATIONAL TAIWAN UNIVERSITY OF SCIENCE AND TECHNOLOGY

RANKING OF NTUST （TIMES HIGHER EDUCATION，THE)



TAIWAN TECH
NATIONAL TAIWAN UNIVERSITY OF SCIENCE AND TECHNOLOGY

RANKING OF NTUST (QS WORLD UNIVERSITY RANKINGS)



TAIWAN TECH NATIONAL TAIWAN UNIVERSITY OF SCIENCE AND TECHNOLOGY

RESEARCH FIELDS

AI / Deep Learning	Biomaterials	Biomedical Electronics and Information	Biomechanics
• Medical image analysis • Computer vision	• Nanomedicine • Biomaterials and Drug Delivery • New drug development	• Biomedical Signals • Biomedical Image Analysis • Ultrasound Molecular Imaging • Biomedical informatics	• Medical Device Research • Gait-analysis • Rehabilitation Engineering • Medical instrumentation

TAIWAN TECH NATIONAL TAIWAN UNIVERSITY OF SCIENCE AND TECHNOLOGY

AWARDS AND HONORS

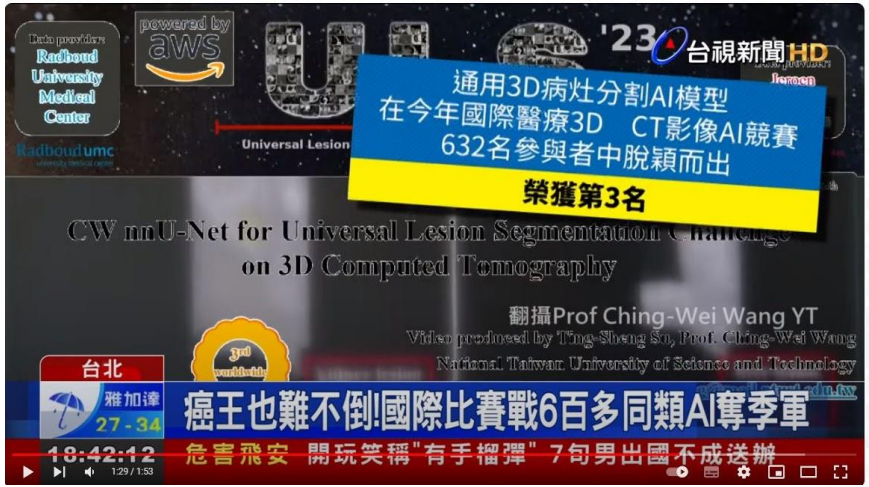
Professor Wang Ching-Wei
1. World's Top 2% Scientists 2023, Stanford University via Scopus, 2024
2. World's Top 2% Scientists 2022, Stanford University via Scopus, 2023
3. World's Top 2% Scientists 2021, Stanford University via Scopus, 2022
4. World's Top 2% Scientists 2020, Stanford University via Scopus, 2021
5. World's Top 2% Scientists 2019, Stanford University via Scopus, 2020

NTUST Reports :
Pioneering AI in Medicine: An Interview with Professor Ching-wei Wang, Director of Biomedical Engineering at Taiwan Tech



TAIWAN TECH
NATIONAL TAIWAN UNIVERSITY OF SCIENCE AND TECHNOLOGY

AWARDS AND HONORS





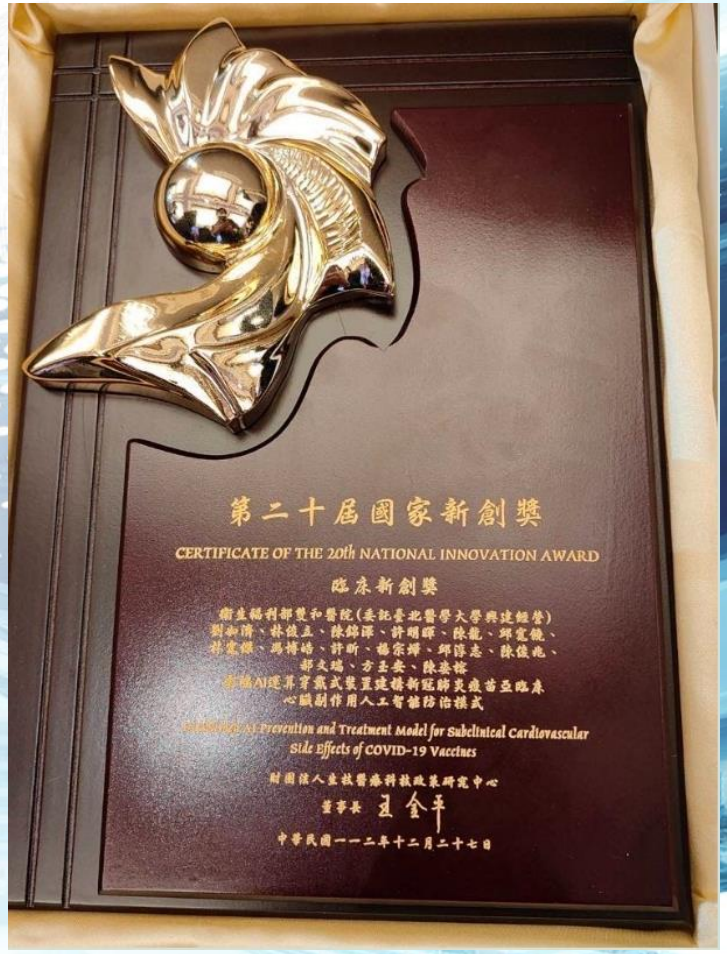


- (3rd place), Universal Lesion Segmentation in Computed Tomography Challenge, Grand Challenge, 2024 April 10th.
- Professor Wang Ching-wei from the Graduate Institute of Biomedical Engineering at National Taiwan University of Science and Technology has developed an AI model that detects tumors in just 2 seconds! This innovation helps avoid the time-consuming and often inaccurate judgments of traditional methods.
- News reports：
  https://www.youtube.com/watch?v=r2CWPNDAQM4&list=PPSV

AWARDS AND HONORS



- Professor Hsu Hsin from the Graduate Institute of Biomedical Engineering at National Taiwan University of Science and Technology and the team led by Professor Liu Ru-ji, Deputy Director of Shuang Ho Hospital, have collaborated to receive recognition at the 20th National Innovation Award!(2023)



AWARDS AND HONORS





- International Award Winning AI platform, 2019 MICCAI Liver Cancer Segmentation challenge, 2019, China
- International Award Winning AI platform, 2019 IEEE ISBI ACDC Automatic Cancer Detection and Classification in Whole-slide Lung Histopathology challenge, 2019 Italy Venice)
- Innovative Invention Award - Super Fast Gigapixel Server , 2018 Taiwan Innotech

TAIWAN TECH
NATIONAL TAIWAN UNIVERSITY OF SCIENCE AND TECHNOLOGY

AWARDS AND HONORS



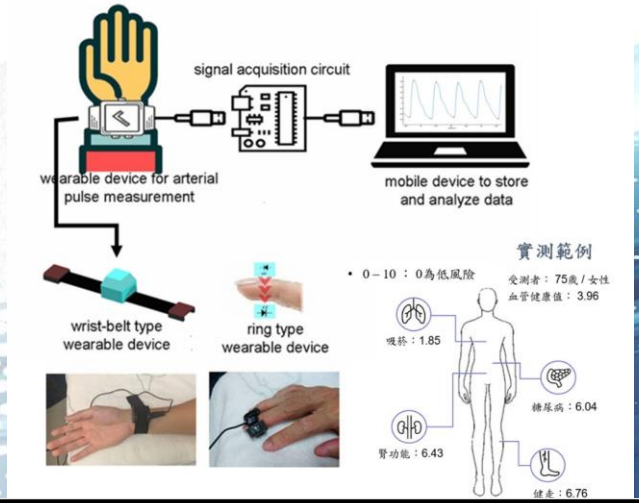
- Taiwan Innotech Expo, 2020



- Prof. Ai-Ho Liao's group won the "2020 Future Tech Breakthrough Award" of the Ministry of Science and Technology.

AWARDS AND NEWS







- Professor Hsu Hsin from National Taiwan University of Science and Technology develops AI wearable device that tests vaccination risks in just one minute.

- News reports：https://youtu.be/vR-XxP90fJs
- News reports： https://www.ntust.edu.tw/p/406-1000-123461,r167.php?Lang=zh-tw

AWARDS AND NEWS



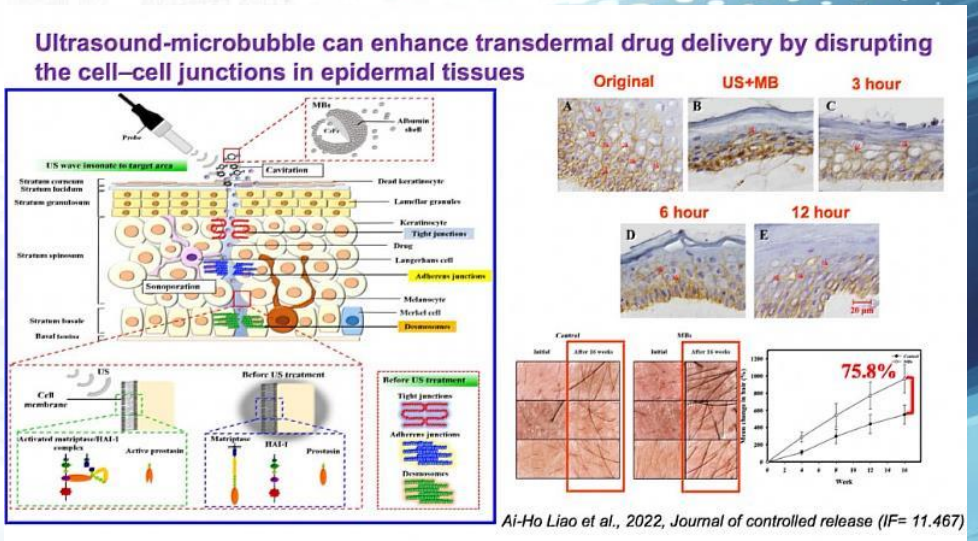


- Professor Hsu Wei-chun from the Graduate Institute of Biomedical Engineering at National Taiwan University of Science and Technology has launched a bilingual sports protection course to cultivate students' practical skills and international.

- News reports：https://www.chinatimes.com/realtimenews/20240907001703-260405?chdtv

AWARDS AND NEWS





- Professor Liao Ai-ho from the Graduate Institute of Biomedical Engineering at National Taiwan University of Science and Technology has developed a microbubble ultrasound needle-free injection system in collaboration with other universities.(2023)
- News reports：
  https://www.cna.com.tw/postwrite/chi/335454

TAIWAN TECH NATIONAL TAIWAN UNIVERSITY OF SCIENCE AND TECHNOLOGY

AWARDS AND NEWS





- Professor Liao Ai-ho from the Graduate Institute of Biomedical Engineering at National Taiwan University of Science and Technology has developed microbubble technology that aids in the creation of a delivery system for COVID-19 medications.(2021)
- News reports：https://www.chinatimes.com/newspapers/20210801000374-260114?chdtv

ADMISSION OF INTERNATIONAL STUDENTS

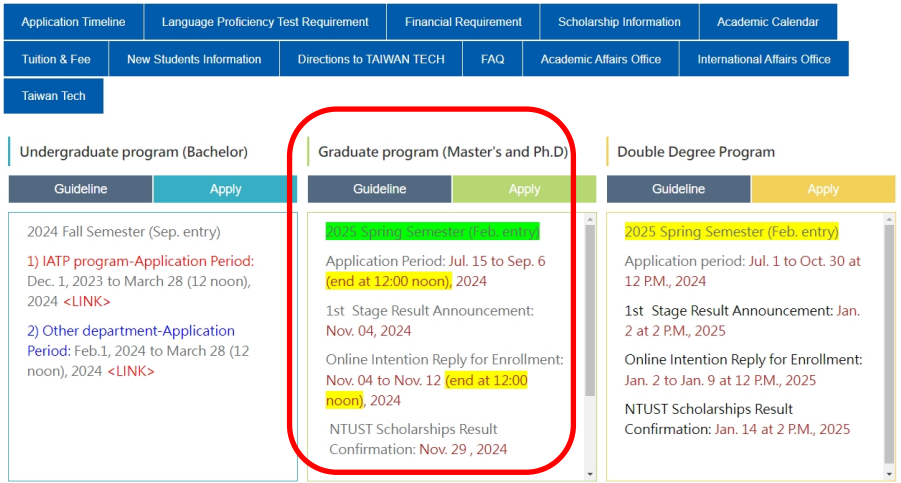
We are recruiting PhD and Master students with Scholarships. Please send Prof Wang your CV, transcript and associated files FIRST.

For PhD positions,

- Please also send your application files to Graduate Institute of Applied Science and Technology through the NTUST university system.
- Apply for NSTC scholarship as suggested (Guide , Detail) or NTUST scholarship.

For Master postitions

- Please also send your application files to Graduate Institute of Biomedical Engineering through the NTUST university system.
- Apply for both NTUST (University Scholarship) and MOE(Ministry of Education, Taiwan) scholarships. (Only one will be granted.)
  - Links: https://sites.google.com/view/chingweiwang/
  - Links: https://admissions.ntust.edu.tw/index/index



2025 Fall Admission Guidelines

- Online application period

  Mar. 7, 2025(end at 12:00 noon)

- Application fee: USD 30(or TWD 1,000) per department/graduate institute.

TAIWAN TECH NATIONAL TAIWAN UNIVERSITY OF SCIENCE AND TECHNOLOGY

ADMISSION OF INTERNATIONAL STUDENTS- REQUIRED DOCUMENTS

- Curriculum Vitae
- Study Plan
- Two Recommendation Letters
- English Proficiency Test:

1. TOEFL(ITP)：585 or above
2. TOEFL(iBT)：85 or above
3. IELTS：6 or above
4. TOEIC Listening and Reading Test：800 or above
5. TOEIC Speaking(170) and Writing Test(165)：335 or above
6. GEPT ：C1 or above
7. Cambridge Main Suite, Linguaskill Business, Linguaskill Business-Speaking, Linguaskill Business-Writing: C1 or above
8. BULATS：67 or above

NTUST SCHOLARSHIPS

Type of Scholarship	Full scholarship		Partial scholarship	
Degree Program	Doctoral	Master	Doctoral	Master
Total	NT$18,000	NT$12,000	NT$12,500	NT$9,000

- Guidelines for National Taiwan University of Science and Technology Scholarships Available to International Graduate Students : https://www.oia.ntust.edu.tw/var/file/60/1060/img/GuidelinesforNTUSTScholarshipsAvailabletoInternationalGraduateStudents(202406ver.).pdf

NSTC SCHOLARSHIP AS SUGGESTED

- For PhD positions
- https://www.nstc.gov.tw/folksonomy/rfpDetail/d896d5d2-d90c-470d-8b61-6efd75677a96



國立臺灣科技大學

TAIWAN TECH

National Taiwan University
of Science and Technology

DEEP LEARNING IN MEDICAL IMAGE ANALYSIS & COMPUTER VISION



TAIWAN TECH NATIONAL TAIWAN UNIVERSITY OF SCIENCE AND TECHNOLOGY

Wang et al. (in press) **Ensemble transformer-based multiple instance learning** to predict pathological subtypes and tumor mutational burden from histopathological whole slide images of endometrial and colorectal cancer, Medical Image Analysis, https://doi.org/10.1016/j.media.2024.103372 (JCR 2023: **IF=10.7**, Q1 3/204 RADIOLOGY, NUCLEAR MEDICINE & MEDICAL IMAGING)

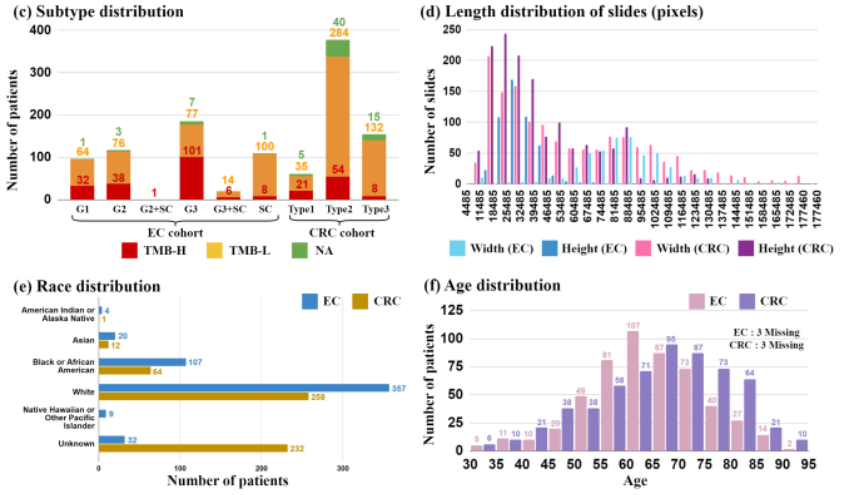
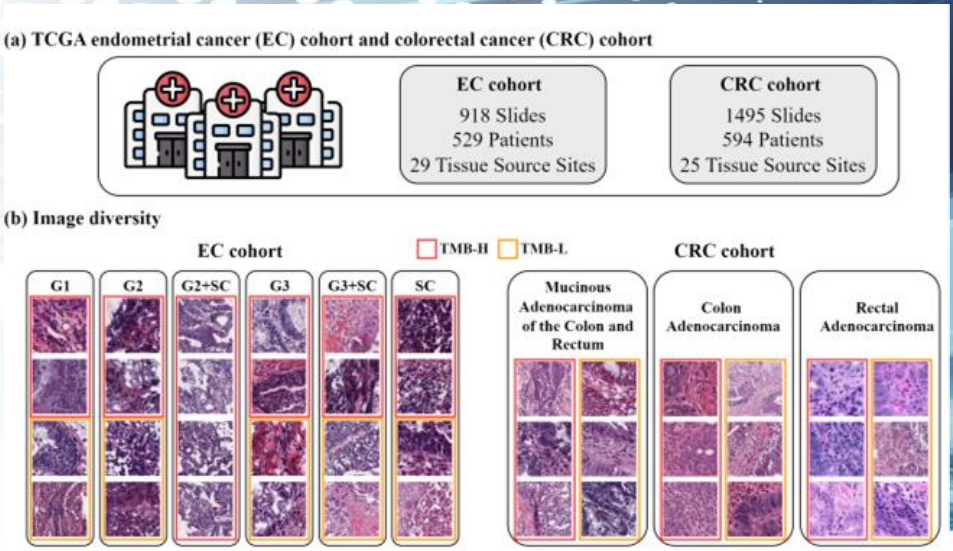


Fig. 4: Data information of two type cancer datasets. (a) TCGA EC cohort and CRC cohort of the data, (b) Image diversity of the data, (c) Subtypes distribution, (d) Length distribution in pixels, (e) Race distribution and (f) Age distribution.



TAIWAN TECH
NATIONAL TAIWAN UNIVERSITY OF SCIENCE AND TECHNOLOGY

DEEP LEARNING IN MEDICAL IMAGE ANALYSIS & COMPUTER VISION

Table 1: Evaluation in Cancer Subtyping and TMB prediction of EC.

Task	Method	Accu.	Prec.	Sens./ Recall	F1-S.	Spec.	MeanSS	MeanSS Rank	AUROC	Fisher Exact Test
(a) EC subtype classification (aggressive vs non-aggressive)	**Proposed ETMIL-SSLViT**	0.86	0.88	0.89	0.88	0.83	0.86	3	**0.92**	**<0.001*** **
	Proposed TMIL-SSLViT	0.87	0.90	0.87	0.88	0.87	0.87	2	**0.92**	**<0.001*** **
	Proposed ETMIL-SSLViT with aug	**0.91**	0.87	**0.99**	**0.92**	0.81	**0.90**	**1**	0.91	**<0.001*** **
	Proposed TMIL-SSLViT with aug	0.84	0.86	0.88	0.87	0.80	0.84	5	0.90	**<0.001*** **
	ClassicMIL Campanella et al. (2019)	0.53	0.61	0.53	0.57	0.53	0.53	11	0.55	0.179
	Wang et al. 2023 Wang et al. (2023d)	0.73	0.78	0.74	0.76	0.72	0.73	9	0.75	**<0.001*** **
	Improved_InceptionV3_MS Wang et al. (2023e)	0.69	0.67	0.90	0.77	0.40	0.65	10	0.80	**<0.001*** **
	CLAM Lu et al. (2021b)	0.83	0.83	0.89	0.85	0.74	0.81	7	0.72	**<0.001*** **
	TOAD Lu et al. (2021a)	0.80	0.88	0.76	0.82	0.86	0.81	7	0.75	**<0.001*** **
	TransMIL Shao et al. (2021)	0.83	**0.92**	0.76	0.83	**0.91**	0.84	5	**0.92**	**<0.001*** **
	MRAN Xiang et al. (2023)	0.86	0.87	0.90	0.88	0.81	0.86	3	0.77	**<0.001*** **
(b) TMB status prediction in the aggressive subtype	**Proposed ETMIL-SSLViT**	**0.77**	**0.70**	0.72	0.71	0.80	0.76	2	0.82	**<0.001*** **
	Proposed TMIL-SSLViT	0.72	0.65	0.61	0.63	0.79	0.70	5	**0.83**	**<0.001*** **
	Proposed ETMIL-SSLViT with aug	**0.77**	0.68	**0.78**	**0.73**	0.77	**0.77**	**1**	0.82	**<0.001*** **
	Proposed TMIL-SSLViT with aug	0.74	0.66	0.69	0.68	0.77	0.73	3	0.81	**<0.001*** **
	ClassicMIL Campanella et al. (2019)	0.61	0.46	0.53	0.49	0.65	0.59	11	0.57	0.127
	Wang et al. 2023 Wang et al. (2023d)	0.74	0.63	0.71	0.67	0.76	0.73	3	0.76	0.436
	Improved_InceptionV3_MS Wang et al. (2023e)	0.70	0.64	0.41	0.50	**0.86**	0.64	9	0.72	**0.017***
	CLAM Lu et al. (2021b)	0.66	0.56	0.67	0.61	0.66	0.66	7	0.70	**0.002****
	TOAD Lu et al. (2021a)	0.64	0.56	0.39	0.46	0.80	0.60	10	0.67	**0.038***
	TransMIL Shao et al. (2021)	0.62	0.51	**0.78**	0.62	0.52	0.65	8	0.63	0.189
	MRAN Xiang et al. (2023)	0.72	0.66	0.58	0.62	0.81	0.70	5	0.77	**<0.001*** **
(c) TMB status prediction in the non-aggressive subtype	**Proposed ETMIL-SSLViT**	**0.66**	**0.50**	0.59	**0.54**	0.69	**0.64**	**1**	0.61	0.181
	Proposed TMIL-SSLViT	0.63	0.46	0.50	0.48	0.69	0.60	2	0.62	0.169
	Proposed ETMIL-SSLViT with aug	**0.66**	**0.50**	0.36	0.42	0.81	0.59	5	0.59	0.213
	Proposed TMIL-SSLViT with aug	**0.66**	**0.50**	0.27	0.35	**0.86**	0.56	7	0.59	0.170
	ClassicMIL Campanella et al. (2019)	0.61	0.41	0.43	0.42	0.70	0.56	7	**0.63**	0.235
	Wang et al. 2023 Wang et al. (2023d)	0.65	0.42	0.25	0.31	0.84	0.54	10	0.54	0.144
	Improved_InceptionV3_MS Wang et al. (2023e)	0.62	0.42	0.55	0.48	0.65	0.60	2	0.58	0.567
	CLAM Lu et al. (2021b)	0.64	0.47	0.41	0.44	0.76	0.59	5	0.42	0.339
	TOAD Lu et al. (2021a)	0.64	0.46	0.48	0.47	0.72	0.60	2	0.55	0.101
	TransMIL Shao et al. (2021)	0.63	0.44	0.36	0.40	0.76	0.56	7	0.56	0.172
	MRAN Xiang et al. (2023)	0.47	0.33	**0.62**	0.43	0.40	0.51	11	0.57	0.567

MeanSS: Mean of Sens. and Spec. The top 1 method are shown in bold format. *:p<0.05, **:p<0.01 and ***:p<0.001

Table 2: Evaluation in Cancer Subtyping and TMB prediction of CRC.

Task	Method	Accu.	Prec.	Sens./ Recall	F1-S.	Spec.	MeanSS	MeanSS Rank	AUROC	Fisher Exact Test
(a) CRC subtype classification (mucinous vs non-mucinous)	**Proposed ETMIL-SSLViT**	0.86	0.41	0.75	0.53	0.87	0.81	3	0.84	**<0.001*** **
	Proposed TMIL-SSLViT	0.89	**0.50**	0.65	**0.57**	0.92	0.79	4	0.83	**<0.001*** **
	Proposed ETMIL-SSLViT with aug	0.87	0.43	0.75	0.55	0.89	**0.82**	**1**	0.86	**<0.001*** **
	Proposed TMIL-SSLViT with aug	0.83	0.36	**0.80**	0.49	0.83	**0.82**	**1**	**0.87**	**<0.001*** **
	ClassicMIL Campanella et al. (2019)	0.73	0.18	0.45	0.26	0.76	0.61	10	0.61	0.056
	Wang et al. 2023 Wang et al. (2023d)	0.69	0.12	0.30	0.17	0.74	0.52	11	0.58	0.429
	Improved_InceptionV3_MS Wang et al. (2023e)	0.61	0.16	0.65	0.26	0.60	0.63	9	0.62	0.344
	CLAM Lu et al. (2021b)	0.87	0.41	0.60	0.49	0.90	0.75	5	0.85	**<0.001*** **
	TOAD Lu et al. (2021a)	0.85	0.37	0.55	0.44	0.89	0.72	6	0.85	**<0.001*** **
	TransMIL Shao et al. (2021)	**0.90**	0.47	0.44	0.46	**0.95**	0.70	8	0.85	**<0.001*** **
	MRAN Xiang et al. (2023)	0.72	0.23	0.70	0.34	0.73	0.71	7	0.78	**<0.001*** **
(b) TMB status prediction in the non-mucinous subtype	**Proposed ETMIL-SSLViT**	0.85	0.46	**0.80**	0.58	0.86	**0.83**	**1**	0.88	**<0.001*** **
	Proposed TMIL-SSLViT	0.80	0.36	0.75	0.48	0.80	0.78	4	0.85	**<0.001*** **
	Proposed ETMIL-SSLViT with aug	0.88	0.52	0.75	**0.61**	0.90	0.82	2	**0.90**	**<0.001*** **
	Proposed TMIL-SSLViT with aug	0.86	**0.47**	0.75	0.58	0.88	0.81	3	0.87	**<0.001*** **
	ClassicMIL Campanella et al. (2019)	0.85	0.00	0.00	0.00	0.98	0.49	11	0.59	1.000
	Wang et al. 2023 Wang et al. (2023d)	0.78	0.16	0.14	0.15	0.88	0.51	7	0.63	0.479
	Improved_InceptionV3_MS Wang et al. (2023e)	0.81	0.15	0.10	0.12	0.92	0.51	7	0.48	0.666
	CLAM Lu et al. (2021b)	0.77	0.19	0.25	0.22	0.85	0.55	5	0.53	0.333
	TOAD Lu et al. (2021a)	0.87	0.00	0.00	0.00	**1.00**	0.50	9	0.67	†
	TransMIL Shao et al. (2021)	0.84	0.27	0.15	0.19	0.94	0.55	5	0.62	0.152
	MRAN Xiang et al. (2023)	**0.89**	0.00	0.00	0.00	**1.00**	0.50	9	0.48	†
(c) TMB status prediction in the mucinous subtype	**Proposed ETMIL-SSLViT**	**0.76**	0.67	**0.86**	**0.75**	0.70	**0.78**	**1**	0.72	0.350
	Proposed TMIL-SSLViT	0.59	0.50	0.57	0.53	0.60	0.59	8	0.65	0.350
	Proposed ETMIL-SSLViT with aug	0.71	0.60	**0.86**	0.71	0.60	0.73	2	0.70	0.350
	Proposed TMIL-SSLViT with aug	0.71	0.60	**0.86**	0.71	0.60	0.73	2	0.67	0.153
	ClassicMIL Campanella et al. (2019)	0.47	0.00	0.00	0.00	0.80	0.40	11	0.43	0.485
	Wang et al. 2023 Wang et al. (2023d)	0.65	0.56	0.71	0.63	0.60	0.66	5	0.67	0.622
	Improved_InceptionV3_MS Wang et al. (2023e)	0.65	0.60	0.43	0.50	0.80	0.61	7	0.77	0.250
	CLAM Lu et al. (2021b)	0.59	0.00	0.00	0.00	**1.00**	0.50	9	**0.90**	†
	TOAD Lu et al. (2021a)	0.65	0.55	**0.86**	0.67	0.50	0.68	4	0.67	0.304
	TransMIL Shao et al. (2021)	0.71	**1.00**	0.29	0.44	**1.00**	0.64	6	0.58	0.154
	MRAN Xiang et al. (2023)	0.35	0.36	0.71	0.48	0.10	0.41	10	0.27	0.537

MeanSS: Mean of Sens. and Spec. The top 1 method are shown in bold format. *:p<0.05, **:p<0.01 and ***:p<0.001
†:No statistics are computed because the model prediction is constant.

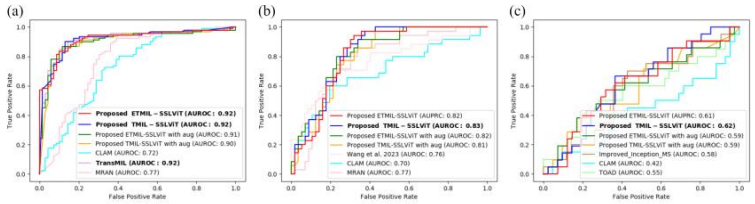


Fig. 2: Area Under the Receiver Operating Characteristic curves (AUROC curves) for assessment of (a) EC subtype classification (aggressive vs non-aggressive), (b) TMB prediction in the aggressive EC subtype (c) TMB prediction in the non-aggressive EC subtype.

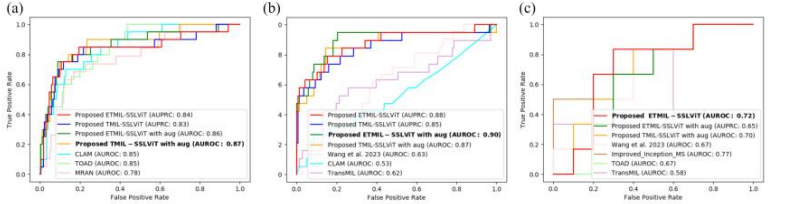
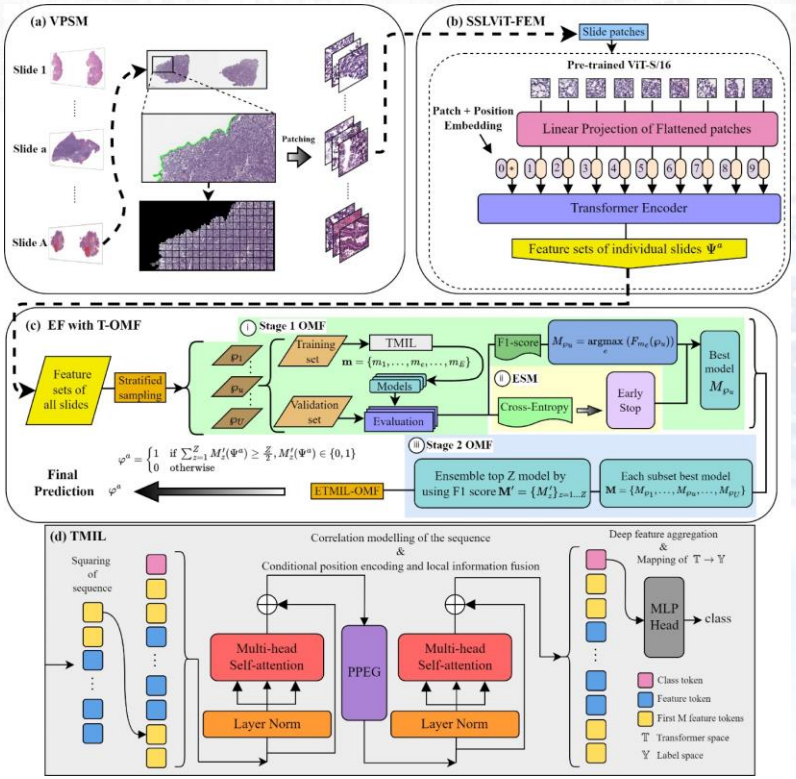


Fig. 3: Area Under the Receiver Operating Characteristic curves (AUROC curves) for assessment of (a) CRC subtype classification (mucinous vs non-mucinous), (b) TMB prediction in the non-mucinous CRC subtype, (c) TMB prediction in the mucinous CRC subtype.

Wang et al. (in press), Medical Image Analysis, https://doi.org/10.1016/j.media.2024.103372 (JCR 2023: **IF=10.7**, Q1 3/204 RADIOLOGY, NUCLEAR MEDICINE & MEDICAL IMAGING)

DEEP LEARNING IN MEDICAL IMAGE ANALYSIS & COMPUTER VISION



1. A highly computational efficient and data efficient DL-framework feasible for clinical usage, which effectively extracts features with feature size as 6% of the original WSI and takes less than three hours for training and less than 30 seconds for inferencing using a cheap GPU card, i.e. GTX 1080 Ti.
2. A Vision Patch Segmentation Module (VPSM) to rapidly extract non-overlapping foreground patches, which helps enhance efficiency and accuracy in WSI analysis.
3. A Self-Supervised Learning Vision Transformer Feature Encoder Module (SSLViT-FEM) that integrates a pre-trained ViT-S/16 with SSL techniques to capture global salient features of images to resolve long-range connections between the content of images and fully utilizes the attention mechanism to incorporate global context information into image features, enhancing the accuracy of the extracted features without significantly increasing computational cost.
4. A Transformer-based Multiple Instance Learning model (TMIL), which outperforms four SOTA MIL methods in this study, establishing its great potential for clinical applications.
5. An Early Stop Mechanism (ESM) to help prevent overfitting and save computational resources and time as Cross Entropy measures the discrepancy between the predicted probability distribution by the model and the actual label distribution, thereby directly reflecting the model's effectiveness in predicting categories.
6. An Ensemble Framework (EF) to improve variance reduction, predictive performance and model robustness and reduce overfitting.

Wang et al. (in press), Medical Image Analysis, https://doi.org/10.1016/j.media.2024.103372 (JCR 2023: **IF=10.7**, Q1 3/204 RADIOLOGY, NUCLEAR MEDICINE & MEDICAL IMAGING)

DEEP LEARNING IN MEDICAL IMAGE ANALYSIS & COMPUTER VISION

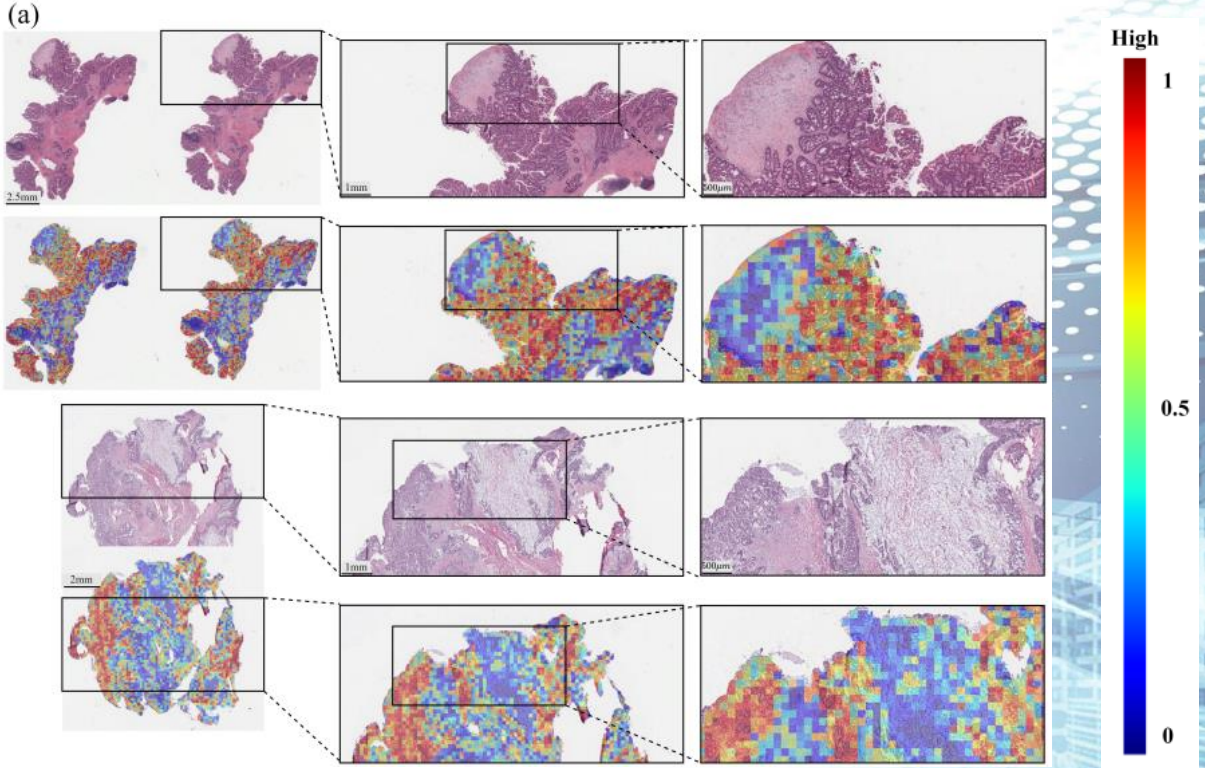


Fig. 5: Model attention heatmaps in prediction of (a) CRC TMB and (b) EC TMB

Wang et al. (in press), Medical Image Analysis, https://doi.org/10.1016/j.media.2024.103372 (JCR 2023: **IF=10.7**, Q1 3/204 RADIOLOGY, NUCLEAR MEDICINE & MEDICAL IMAGING)

DEEP LEARNING IN MEDICAL IMAGE ANALYSIS & COMPUTER VISION

Table 6: Run time analysis of the proposed framework using different SSL-based backbones

		(a) Data size (MB / slide)		(b) Run time in feature extraction (seconds / slide)	
SSL method	Backbone	File size	Feature size	Create patches	Extract features
BT	ResNet-50	287.55	96.88	3.14	22.14
MoCoV2		287.55	96.88	3.14	22.65
SwAV		287.55	96.88	3.14	22.41
DINO	ViT-S/8	287.55	18.16	3.14	23.07
DINO (Proposed)	ViT-S/16	287.55	18.16	3.14	23.62

		(c) Run time in AI inference (seconds / slide)		(d) AI training (minutes)		
SSL method	Backbone	Inference (c1)	Total inference time (c1+b)	(d1) Training per epoch	(d2) Max 200 epochs with early stop	Total training time (d2+b)
BT	ResNet-50	0.06	25.34	0.45	28	165
MoCoV2		0.06	25.84	0.80	31	171
SwAV		0.06	25.61	0.80	30	169
DINO	ViT-S/8	0.04	26.24	0.76	19	161
DINO (Proposed)	ViT-S/16	0.04	26.80	0.75	17	163

curacy (87%), respectively. In addition, we evaluated the computational efficiency of individual backbones to compare the feature size, runtime in model training and inference on a workstation equipped with an affordable GPU (NVIDIA GTX 1080 Ti) with 12 gigabytes of memory, a CPU (Intel Core i9-7900X),

file size 287.55 MB, ResNet50 series generates the largest feature size (96.88 MB), while the ViT series effectively extracts the smallest feature size (18.16 MB). On the other hand, ViT series takes around 0.4 to 1 second more per slide for feature extraction and so as for AI inference. For AI training, the proposed framework with any one of the five SSL-based backbones takes less than three hours for training, and the runtime analysis also shows that our architecture converges faster using DINO-ViT backbones with the lowest total training time among all.

Wang et al. (in press), Medical Image Analysis, https://doi.org/10.1016/j.media.2024.103372 (JCR 2023: **IF=10.7**, Q1 3/204 RADIOLOGY, NUCLEAR MEDICINE & MEDICAL IMAGING)

DEEP LEARNING IN MEDICAL IMAGE ANALYSIS & COMPUTER VISION

Data Availability

The data that support the findings of this study are publicly available online through the TCGA's Genomic Data Commons (https://portal.gdc.cancer.gov/) with the project ID as TCGA-UCEC for EC dataset and (TCGA-COAD and TCGA-READ) for CRC dataset. The exact case IDs and associated labels can be accessed on the following links, (EC-labels) for EC dataset and (CRC-labels) for CRC dataset. Full clinical information could be downloaded from (Uterine Corpus Endometrial Carcinoma (TCGA, PanCancer Atlas)) and (Colorectal Adenocarcinoma (TCGA, PanCancer Atlas)).

Code Availability

The proposed DL model was deployed using the Pytorch framework in Python and the program code has been made publicly accessible on GitHub (https://github.com/cwwang1979/ETMIL-OMF) (For reviewers, please use the password to unzip the program file: ji32k7au4a83_cwlab).

Wang et al. (in press) Ensemble transformer-based multiple instance learning to predict pathological subtypes and tumor mutational burden from histopathological whole slide images of endometrial and colorectal cancer, Medical Image Analysis, https://doi.org/10.1016/j.media.2024.103372 (JCR 2023: **IF=10.7**, Q1 3/204 RADIOLOGY, NUCLEAR MEDICINE & MEDICAL IMAGING)

DEEP LEARNING IN MEDICAL IMAGE ANALYSIS & COMPUTER VISION

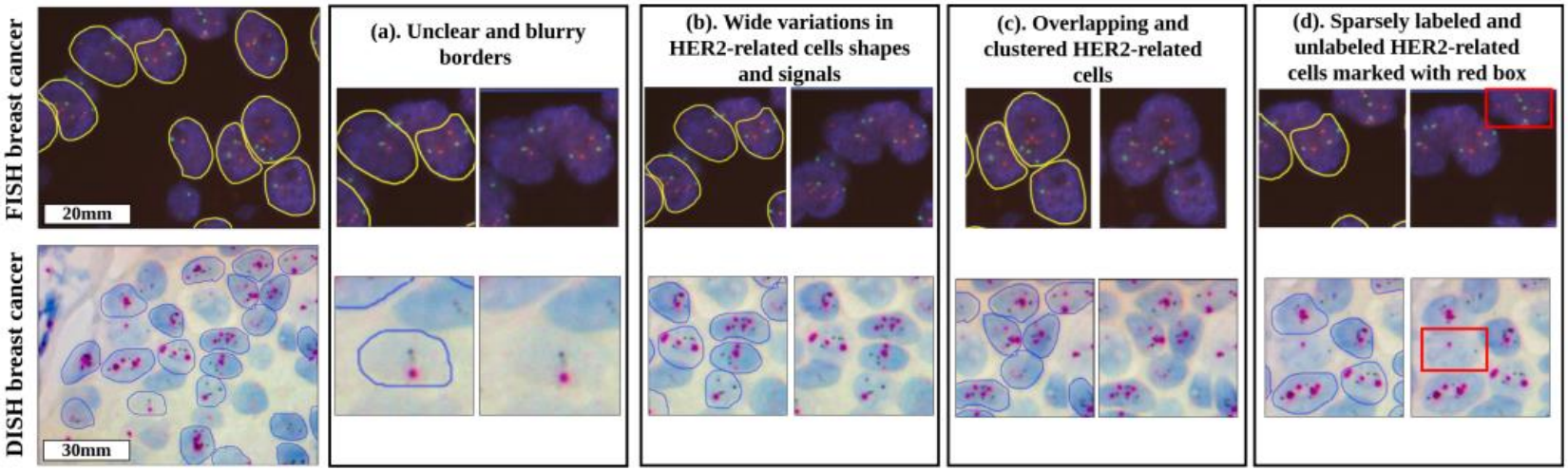


Fig. 1. Challenges in FISH and DISH image analysis. (Left) Partial views of a FISH and DISH image with annotations by trained pathologists. (a) Unclear and blurry cell boundaries, (b) Wide variations in HER2-related cell shapes and signals, (c) Overlapping and clustered HER2-related cells, and (d) Sparse annotation with some unlabeled HER2-related cells marked with the red box.

Wang et al. (in press) Automated quantification of HER2 amplification levels using deep learning, IEEE Journal of Biomedical and Health Informatics , DOI: 10.1109/JBHI.2024.3476554 (JCR 2023: **IF= 6.7**, Q1 3/44 MEDICAL INFORMATICS) [First author]

TAIWAN TECH NATIONAL TAIWAN UNIVERSITY OF SCIENCE AND TECHNOLOGY

DEEP LEARNING IN MEDICAL IMAGE ANALYSIS & COMPUTER VISION

TABLE I

DATA DISTRIBUTION OF THE THREE CLINICAL DATA SETS

(a) Breast cancer

Data	Mag.	Size (pixels)	Total	Training(70%)		Testing(30%)
				Training(90%)	Validation(10%)	
FISH	600×	1360×1024	200	120	14	66
DISH	1200×	1600×1200	210	132	16	62

(b) Stomach cancer

Data	Mag.	Size (pixels)	Total	Training(50%)		Testing(50%)
				Training(90%)	Validation(10%)	
DISH	600×	1360×1024	45	20	3	14
		4080×3072		0	0	8

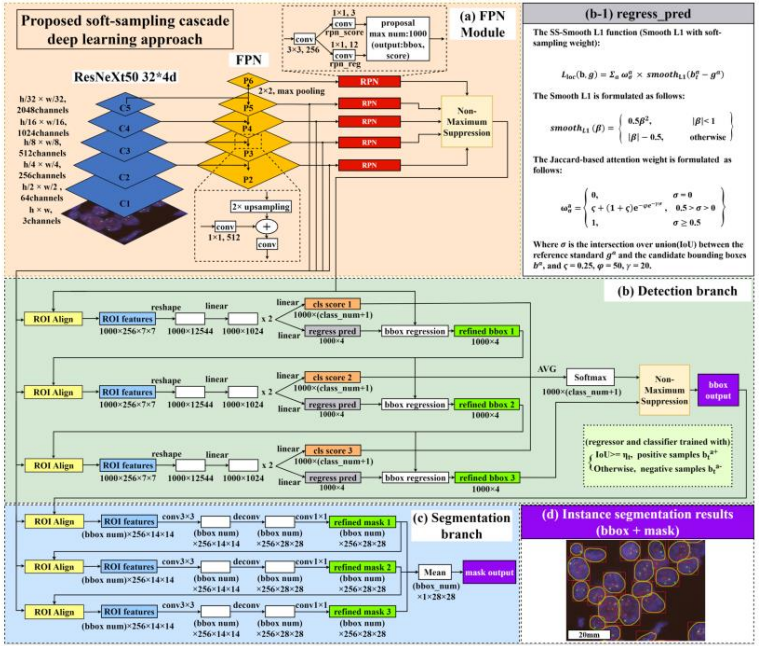
We selected patients who came to the hospital for breast cancer therapy with invasive ductal carcinoma pathology diagnosis for FISH or DISH imaging of metastatic breast cancer. From January 2014 to December 2021, dual-color FISH and DISH images in HER2 IHC score 2+ equivocal cases were de-identified and digitized. Two trained examiners analyzed the DISH and FISH data individually, producing annotations of particular cancerous cells with related labels of HER2 and CEN17 signals.

A. Materials

De-identified and digitized 410 breast cancer images, including 200 FISH images and 210 DISH images with reference standard generated by the experienced pathologists were obtained from the tissue bank of the Department of Pathology, Tri-Service General Hospital, National Defense Medical Center, Taipei, Taiwan. The research ethics board of the Tri-Service General Hospital approved the ethical approval (TSGHIRB 1-107-05-171, B2020-050-70). The slides for the FISH breast data were captured at 600× overall magnification with a 10× eyepiece lens (Olympus, Japan) and a 60× objective lens (Olympus, Japan) and for the DISH breast data were reproduced at 1200× overall magnification with a 20× eyepiece lens (Olympus, Japan) and a 60× objective lens (Olympus, Japan). The data distribution of two clinical data sets are based on the previously published paper to ensure fair comparison [27] (see Table I(a) for detailed information). To test whether DL-based prediction of HER2 amplification can also be applied to gastric cancer patients, we collected 45 de-identified and digitized gastric cancer DISH images. The slides for the DISH gastric cancer data were captured at 600× total magnification using a 10× eyepiece lens (Olympus, Japan) and a 60× objective lens (Olympus, Japan)(Table I(b)).

Wang et al. (in press) Automated quantification of HER2 amplification levels using deep learning, IEEE Journal of Biomedical and Health Informatics, DOI: 10.1109/JBHI.2024.3476554

DEEP LEARNING IN MEDICAL IMAGE ANALYSIS & COMPUTER VISION



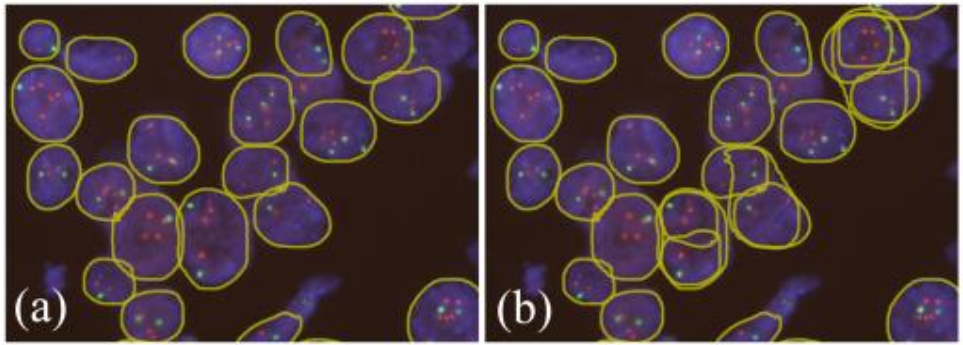


Fig. 4. Over-segmentation issue. Compare different IoU threshold (a) $\mu = 0.4$ and (b) $\mu = 0.5$.

Fig. 2. The main architecture of the proposed method. (a) The FPN module with orange background color shows two concepts of top-down sampling and skip-connection to extract the intermediate convolutional feature ζ using ResNeXt50 as the backbone network. Then, the features ζ are transferred into the RPN module to generate the bounding box prediction $\{\mathbf{b}_t^a\}_{t=1..T}$ and then moved into the (b) Detection branch part with the green background color to generate the final bounding box result $\mathbf{b}_*^a$. (b-1) Our proposed soft-sampling weighted loss function generates the new bounding box feature regression equations. (c) Segmentation branch area with blue background color aims to pass the final prediction bounding boxes $\mathbf{b}_*^a$ into the segmentation branch to generate the final prediction masks $\mathbf{m}_*^a$. (d) Instance segmentation results by the proposed method.

DEEP LEARNING IN MEDICAL IMAGE ANALYSIS & COMPUTER VISION

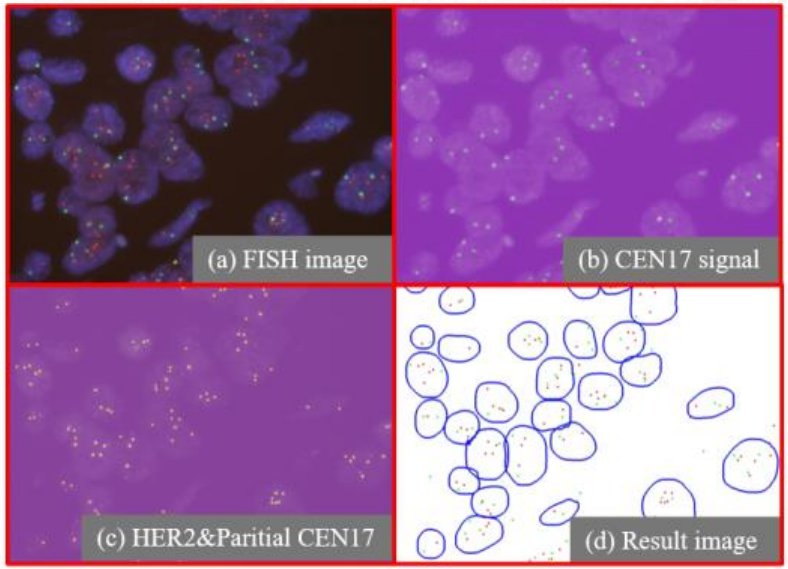


Fig. 5. CEN17 and HER2 signal detection result on FISH data set. (a) a raw FISH image sample, (b) CEN17 signal detection results highlighted in green using equation 31, (c) results of signal detection of HER2 and partial CEN17, highlighted in yellow, using equation 32 and (d) detection results of CEN17, HER2 and HER2 related cells by the proposed method highlighted in green, red and blue, respectively.

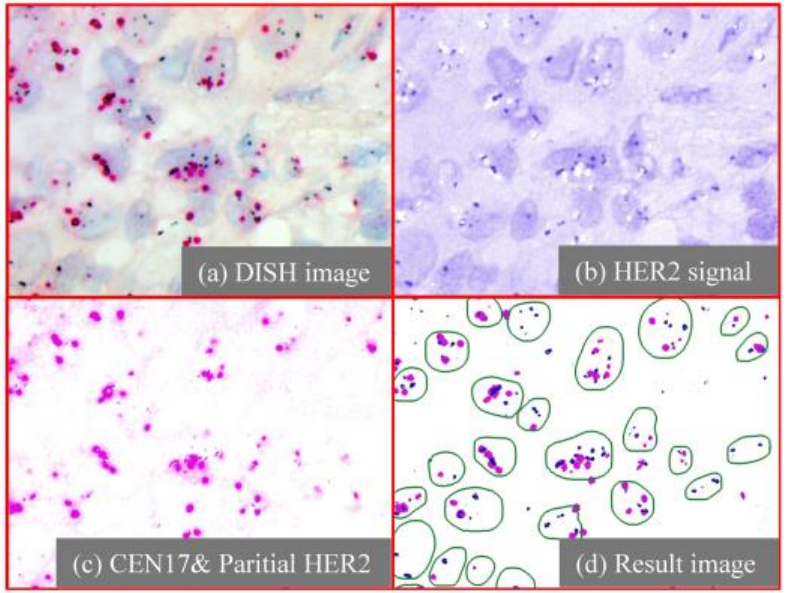


Fig. 6. CEN17 and HER2 signal detection result on DISH data set. (a) a raw DISH image sample , (b) HER2 signal detection results highlighted in blue using equation 33, (c) results of signal detection of CEN17 and partial HER2, highlighted in pink, using equation 33 and (d) detection results of HER2, CEN17 and HER2 related cells by the proposed method highlighted in blue, pink and green, respectively.

Wang et al. (in press) Automated quantification of HER2 amplification levels using deep learning, IEEE Journal of Biomedical and Health Informatics, DOI: 10.1109/JBHI.2024.3476554

DEEP LEARNING IN MEDICAL IMAGE ANALYSIS & COMPUTER VISION

TABLE II

QUANTITATIVE EVALUATION FOR HER2-RELATED CELL SEGMENTATION ON MICROSCOPE DATA SETS.

(a) FISH breast cancer dataset

Method	Backbone	Accuracy (%)	Precision (%)	Recall (%)	F1-score (%)	Jaccard-Index (%)	AJI (%)	AJI_{sparse} (%)	F1-score Rank
Proposed Method	**ResNeXt-50(32*4d)**	**98.74±1.32**	**99.5±0.74**	**95.32±4.68**	**97.31±2.65**	**94.88±4.83**	**57.55±8.51**	**70.67±7.06**	**1**
CPN [28]	ResNet-50	77.67±8.38	57.55±8.46	76.95±8.03	65.35±6.72	48.46±7.37	8.05±5.95	20.22±11.69	10
SL-FCN [27]	-	93.54±5.25	91.75±8.27	83.53±13.15	86.98±9.86	78.22±14.73	6.77±5.81	15.17±9.98	3
Modified FCN [18]	-	93.38±4.46	91.9±7.87	82.13±10.99	86.41±8.38	76.97±12.5	7.36±6.5	15.76±10.49	4
Contour_BCNet$^{\Psi}$ [29]	ResNet-50	93.56±4.61	99.24±1.12	76.43±13.65	85.67±9.9	76.09±13.71	52.51±10.41	59.9±10.53	5
BBox_BCNet$^{\Psi}$ [29]	ResNet-50	85.98±5.58	83.27±8.11	62.36±12.08	70.55±9.77	54.8±10.79	13.97±6.3	23.66±8.51	8
SOLOv2 [30]	ResNet-50	88.11±4.48	79.55±8.01	75.86±6.6	77.38±5.82	62.94±7.45	12.03±8.42	24.71±12.41	6
Deeplabv3+ [33]	MobileNet [37]	85.17±5.18	75.53±6.14	64.94±9.99	69.36±7.27	53.55±8.08	7.2±3.96	10.29±5.77	9
Deeplabv3+ [33]	ResNet-101 [38]	85.06±5.23	69.79±7.3	76.44±9.28	72.52±6.62	57.29±7.65	6.1±4.08	12.1±7.61	7
Deeplabv3+ [33]	Xception [39]	76.83±11.67	66.35±19.82	45.27±24.82	47.55±20.44	33.73±15.58	3.84±4.19	6.01±6.07	11
Cascade R-CNN [32]	ResNet-101	94.69±3.56	97.98±2.31	81.1±10.61	88.38±7.45	79.87±10.71	47.27±8.68	56.75±9.13	2

(b) DISH breast cancer dataset

Method	Backbone	Accuracy (%)	Precision (%)	Recall (%)	F1-score (%)	Jaccard-Index (%)	AJI (%)	AJI_{sparse} (%)	F1-score Rank
Proposed Method	**ResNeXt-50(32*4d)**	**95.03±3.47**	**97.42±3.07**	**82.62±12.07**	**88.98±8.25**	**81.06±12.42**	**44.89±11.34**	**58.37±10.57**	**1**
CPN [28]	ResNet-50	75.94±7.55	65.94±12.11	57.13±17.11	59.37±12	43.21±12.06	11.09±8.7	23.54±13.14	8
SL-FCN [27]	-	87.77±14.97	77.19±23.41	91.2±7.72	81.67±17.76	72.4±23.05	6.82±8.34	17.11±15.77	2
Modified FCN [18]	-	91.26±7.57	83.13±11.33	71.6±15.39	75.79±11.39	62.4±15.43	18.19±11.06	31.27±12.05	4
Contour_BCNet $^{\Psi}$ [29]	ResNet-50	87.32±8.17	97.7±2.55	58.1±18.92	71.1±15.45	57.33±18.61	39.78±14.27	46.48±15.13	6
BBox_BCNet$^{\Psi}$ [29]	ResNet-50	83.71±6.28	76.21±12.4	62.34±14.3	67.44±11.08	51.91±12.45	9.3±6.8	18.13±10.53	7
SOLOv2 [30]	ResNet-50	84.37±6.34	76.82±7.32	70.24±15.33	72.34±10.01	57.56±11.79	16.71±13.55	31.68±17.92	5
Cascade R-CNN [32]	ResNet-101	90.69±5.62	97.48±3.92	66.05±18.35	77.22±14.62	65.02±18.38	43.15±13.65	49.96±14.04	3

(c) DISH stomach cancer dataset

Method	Backbone	Accuracy (%)	Precision (%)	Recall (%)	F1-score (%)	Jaccard-Index (%)	AJI (%)	AJI_{sparse} (%)
Proposed Method	ResNeXt-50(32*4d)	97.67±1.46	96.15±5.82	77.83±8.94	85.82±6.95	75.77±10.46	27.52±7.89	55.48±8.2

$^{\Psi}$ The method of BCNet which use bounding bbox and contour as annotation to train the model, respectively.

AJI : Aggregated Jaccard Index ; AJI_{sparse} : Aggregated Jaccard Index excludes unlabeled cells from the evaluation.

Wang et al. (in press) Automated quantification of HER2 amplification levels using deep learning, IEEE Journal of Biomedical and Health Informatics, DOI: 10.1109/JBHI.2024.3476554

TAIWAN TECH NATIONAL TAIWAN UNIVERSITY OF SCIENCE AND TECHNOLOGY

DEEP LEARNING IN MEDICAL IMAGE ANALYSIS & COMPUTER VISION

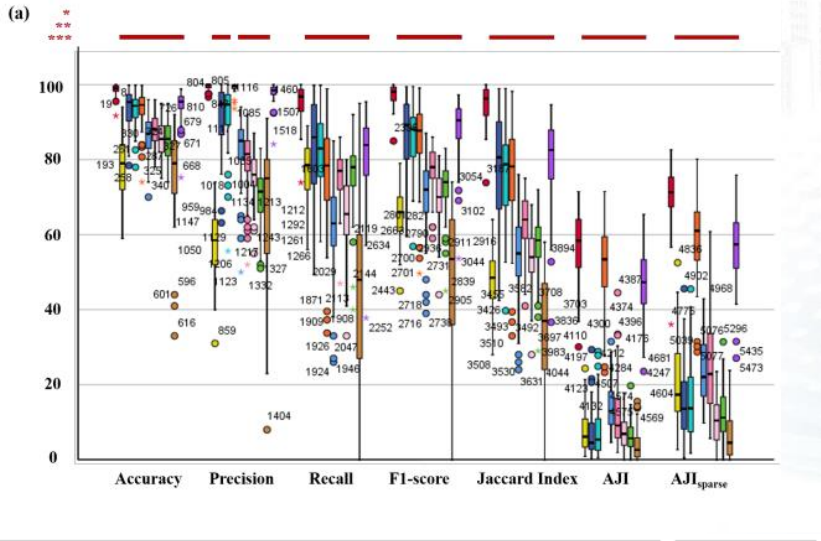
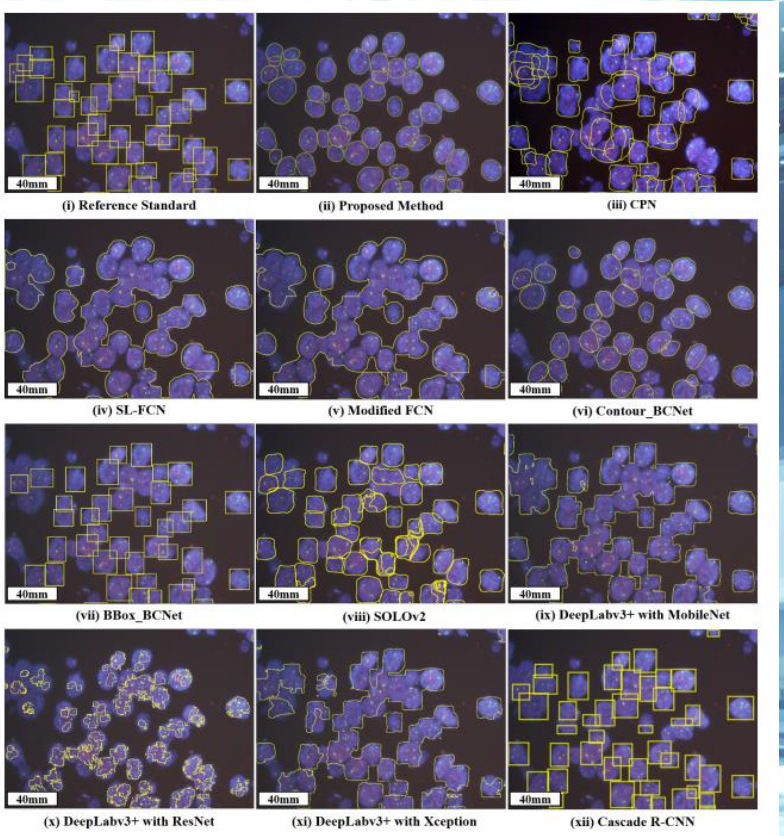


Fig. 7. The box plots of quantitative evaluation results on the two breast cancer datasets, including (a) FISH fluorescent microscope data set and (b) DISH light microscope data set.



Wang et al. (in press) Automated quantification of HER2 amplification levels using deep learning, IEEE Journal of Biomedical and Health Informatics, DOI: 10.1109/JBHI.2024.3476554

TAIWAN TECH NATIONAL TAIWAN UNIVERSITY OF SCIENCE AND TECHNOLOGY

DEEP LEARNING IN MEDICAL IMAGE ANALYSIS & COMPUTER VISION

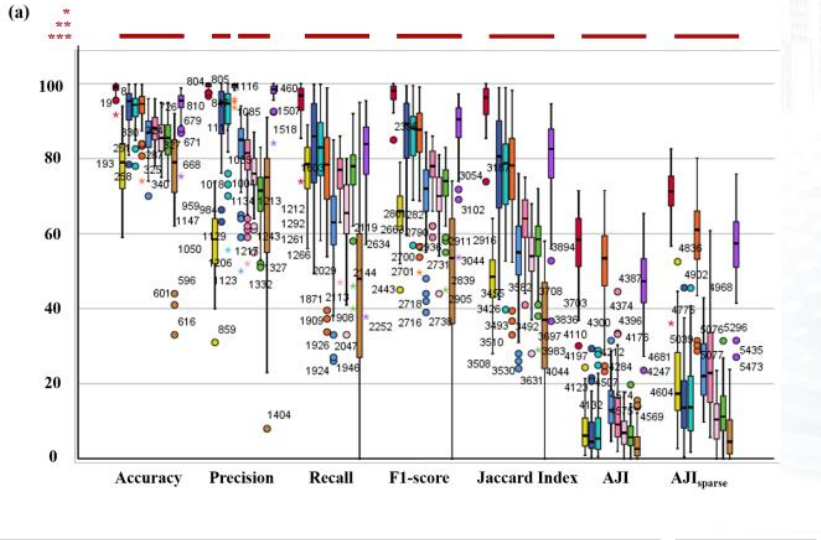
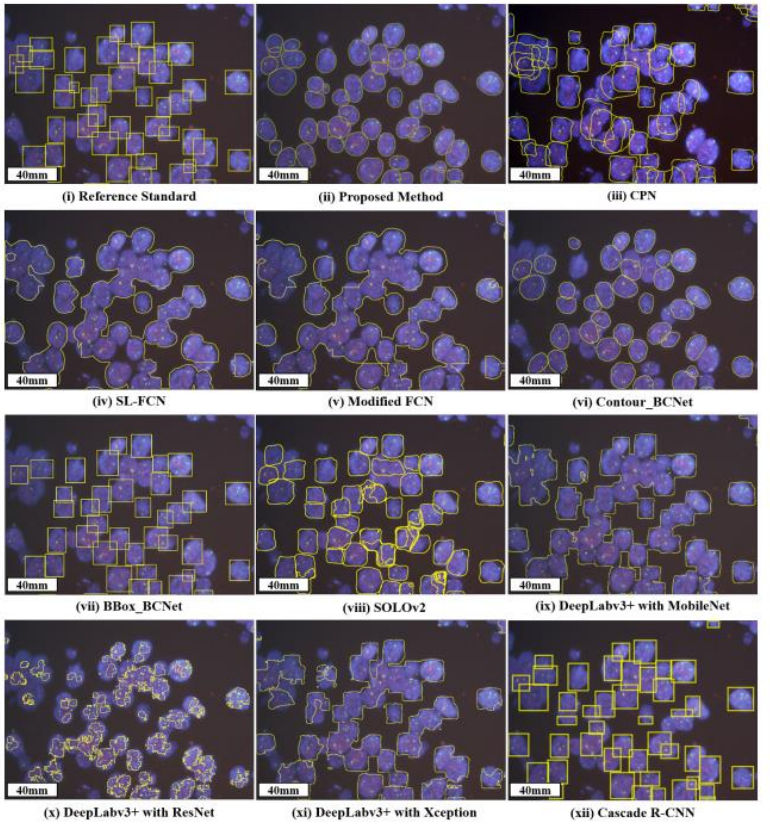


Fig. 7. The box plots of quantitative evaluation results on the two breast cancer datasets, including (a) FISH fluorescent microscope data set and (b) DISH light microscope data set.



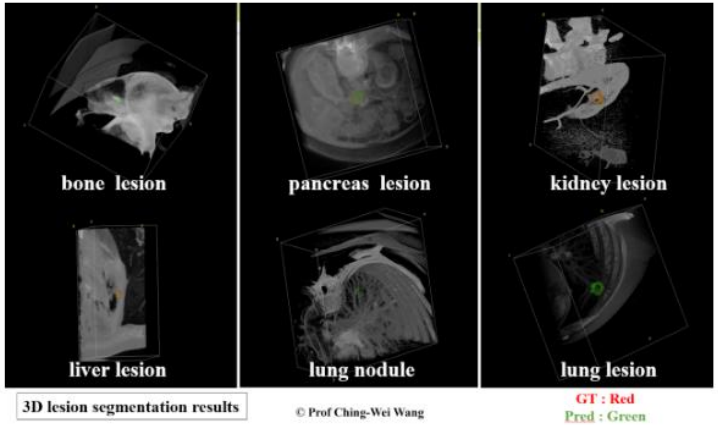
Wang et al. (in press) Automated quantification of HER2 amplification levels using deep learning, IEEE Journal of Biomedical and Health Informatics, DOI: 10.1109/JBHI.2024.3476554

TAIWAN TECH NATIONAL TAIWAN UNIVERSITY OF SCIENCE AND TECHNOLOGY

DEEP LEARNING IN MEDICAL IMAGE ANALYSIS & COMPUTER VISION

Professor Wang Ching-Wei Develops Universal 3D Lesion Segmentation AI Model

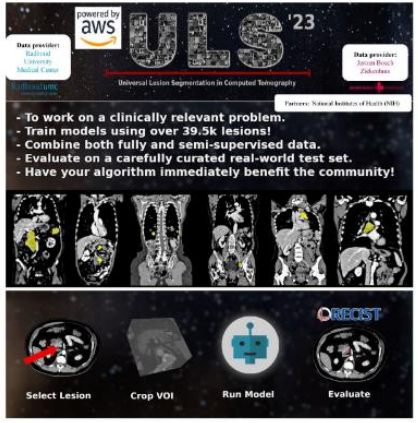
Automated AI lesion segmentation for CT scans offers significant advantages over manual segmentation, such as improved efficiency, repeatability, accuracy, and standardization, leading to more precise quantitative analysis. Traditional manual annotation takes about 30 to 60 minutes per case, whereas Professor Wang's model can process each 3D lesion in equipped with an RTX 4080]. just 3.25 seconds [on the Grand Challenge platform server equipped with a single T4 GPU, and less than 2 seconds on a computer



3D lesion segmentation results

© Prof Ching-Wei Wang

GT : Red
Pred : Green





CW nnU-Net ranks as the **3rd place**

TAIWAN TECH
NATIONAL TAIWAN UNIVERSITY OF SCIENCE AND TECHNOLOGY

DEEP LEARNING IN MEDICAL IMAGE ANALYSIS & COMPUTER VISION



Car, License Plate, and People Detection with Face Detection

觀看次數：81次・4 年前



Car, License Plate, and People Detection-2

觀看次數：77次・4 年前



Car, License Plate, and People Detection-1

觀看次數：57次・4 年前



Car, License Plate, and People Detection-3

觀看次數：39次・4 年前



Car Type, Car Color, Car Brand Recognition with NX Witness

觀看次數：336次・4 年前



Vehicle, Car, Motorbike, People Detection with NX Witness

觀看次數：176次・4 年前



Car Plate Recognition with NX Witness

觀看次數：256次・4 年前



Auto License Plate Recognition in Night 人工智慧即時自動車牌辨識 夜晚

觀看次數：145次・5 年前



Auto License Plate Recognition in Rainy Day 人工智慧即時自動車牌辨識 雨天

觀看次數：147次・5 年前



Auto License Plate Recognition in Heavy Rainy Day 人工智慧即時自動車牌辨識 大雨天

觀看次數：106次・5 年前



Vehicle Type and Pedestrian Detection Multiview 人工智慧即時行車種類辨識與行...

觀看次數：148次・5 年前



Vehicle Type and Pedestrian Detection in Rainy Day 人工智慧即時行車種類辨識與行...

觀看次數：99次・5 年前

TAIWAN TECH
NATIONAL TAIWAN UNIVERSITY OF SCIENCE AND TECHNOLOGY

Q&A